

*Citation for published version:*

Alafnan, H, Zhang, M, Yuan, W, Zhu, J, Li, J, Elshiekh, M & Li, X 2018, 'Stability Improvement of DC Power Systems in an All-Electric Ship Using Hybrid SMES/Battery', *IEEE Transactions on Applied Superconductivity*, vol. 28, no. 3, 5700306, pp. 1-6. <https://doi.org/10.1109/TASC.2018.2794472>

*DOI:*

[10.1109/TASC.2018.2794472](https://doi.org/10.1109/TASC.2018.2794472)

*Publication date:*

2018

*Document Version*

Peer reviewed version

[Link to publication](#)

*Publisher Rights*

Unspecified

© 2018 IEEE. Personal use of this material is permitted. Permission from IEEE must be obtained for all other users, including reprinting/ republishing this material for advertising or promotional purposes, creating new collective works for resale or redistribution to servers or lists, or reuse of any copyrighted components of this work in other works.

**University of Bath**

## **Alternative formats**

If you require this document in an alternative format, please contact:  
[openaccess@bath.ac.uk](mailto:openaccess@bath.ac.uk)

**General rights**

Copyright and moral rights for the publications made accessible in the public portal are retained by the authors and/or other copyright owners and it is a condition of accessing publications that users recognise and abide by the legal requirements associated with these rights.

**Take down policy**

If you believe that this document breaches copyright please contact us providing details, and we will remove access to the work immediately and investigate your claim.

# Stability Improvement of DC Power Systems in an All-Electric Ship Using Hybrid SMES/Battery

Hamoud Alafnan, Min Zhang, Weijia Yuan, Jiahui Zhu, Jianwei Li, Mariam Elshiekh and Xiaojian Li

**Abstract**—As the capacity of all-electric ships (AES) increases dramatically, the sudden changes in the system load may lead to serious problems, such as voltage fluctuations of the ship power grid, increased fuel consumption and environmental emissions. In order to reduce the effects of system load fluctuations on system efficiency, and to maintain the bus voltage, we propose a hybrid energy storage system (HESS) for use in AESs. The HESS consists of two elements: a battery for high energy density storage and a superconducting magnetic energy storage (SMES) for high power density storage. A dynamic droop control is used to control charge/discharge prioritisation. Manoeuvring and pulse loads are the main sources of the sudden changes in AESs. There are several types of pulse loads, including electric weapons. These types of loads need large amounts of energy and high electrical power, which makes the HESS a promising power source. Using Simulink/Matlab, we built a model of the AES power grid integrated with a SMES/battery to show its effectiveness in improving the quality of the power grid.

**Index Terms**—All-electric ship (AES), hybrid energy storage system (HESS), superconducting magnetic energy storage (SMES), pulse load.

## I. INTRODUCTION

As the world trending to be electric, ship technology is no exception. In the past, ship design did not depend mainly on the electrical power system because ships were propelled mechanically by connecting the steam engines or turbines directly to the propellers. However, the introduction of ships that were propelled electrically opened the door for the increased inclusion of electrical design in shipbuilding. To encourage the trend to electrification, the concept of all-electric ship (AES) was proposed by the U.S. Navy [1]. As the capacity of the AES

is expected to reach hundreds of megawatts in the near future [2], a high-performance power system with multiple power sources is required to meet such huge power demands. The AES has different types of loads, including propulsion loads, ship service loads and pulse loads, such as electrical weapons. Electrical weapons rely on stored energy to attack targets, which need a high amount of power in a short period.

On the AES design, one of the most important features is the ramp-rate of the generators. The ramp-rate is the increased or decreased rate of the output power per minute and usually in MW/minute. The ramp-rate of ships' generators, such as gas-turbine generators are in the range of 35 to 50 MW/minute, whereas the pulse loads required a 100 MW/second ramp-rate, which is significantly higher than the ramp-rate of the generators [3], [4]. If the changes in the loads are faster than the ramp rate of the generators, unbalanced power between loads and generators occurs, which leads to instability in the power system. Because the ramp-rate of the ship's generators is not high enough to maintain the power demanded by electrical weapons, the need for an integrated power system (IPS) architecture is inevitable. The IPS is intended to provide the total amount of power required by the AES by using common set of sources [5]. Missions that require high power support, such as a weaponry system and improve the efficiency of propulsion, which are some of the advantages of the use of an IPS in ships [6]. IEEE 1709 recommends the use of medium-voltage DC (MVDC) in shipboard power systems, which improves the reliability, survivability and power quality of the system [7].

The hybrid SMES/Battery has been proposed for railway substations by using fuzzy control [8]. The use of the SMES was proposed in a hybrid vehicle in which a cryogenic tank already existed [9]. A SMES/Battery hybrid energy storage system (HESS) was integrated into microgrids to mitigate the influence of the renewable generations [10]. The implementation of a HESS for AESs has been proposed to supply both the peak and pulsed loads. Several studies were performed to mitigate the effects of the pulse loads on shipboard power system by using HESS. A supercapacitor and batteries were combined to supply pulse loads and support grid stability with different control schemes [11], [12]. A flywheel energy storage system was added to the system to maintain the health of the ship's power systems by maintaining the propulsion motor speed and the generator speed during pulse load periods [13].

Manuscript receipt and acceptance dates will be inserted here.

Hamoud Alafnan would like to thank the University of Hail studentship. Min Zhang would like to thank RAEng Research Fellowship. This work was partly supported by the China State Grid Corporation Science and Technology Project under Grant No. DG71-16-002, DG83-17-002, DG71-17-020. (Corresponding author: Min Zhang.)

H. Alafnan, M. Zhang, W. Yuan, and M. Elshiekh are with the Department of Electronic and Electrical Engineering, University of Bath, Bath BA2 7AY, UK (e-mail: m.zhang2@bath.ac.uk).

J. Zhu is with the China Electric Power Research Institute, No.15 Xiaoying Rd(E), Qinghe, Beijing 100192, China.

J. Li is with the Department of the Electrical Engineering & Computer Science, University of Liege, 4000 Liege, Belgium.

X. Li, is with the China North Vehicle Institute, No. 4 Huaishuling, Fengtai District, Beijing, China.

Color versions of one or more of the figures in this paper are available online at <http://ieeexplore.ieee.org>.

Digital Object Identifier will be inserted here upon acceptance.

In this paper, we propose the use of the superconducting magnetic energy storage (SMES)/battery HESS in AESs. Compared with supercapacitors, flywheels, and other energy storage devices, SMES devices have higher power density, faster time response and unlimited charge and discharge life cycles [14], [15]. Because the battery has a relatively low power density [16], it cannot respond quickly in supplying the high transient current that is needed for the pulse loads. In this model, SMES works as a high power density device and a battery as the high energy density device. A dynamic droop control is used to coordinate the charge/discharge prioritisation between the SMES and the battery. The ultimate goal of the HESS, based on dynamic droop control, is to supply the power demanded by the pulse loads and to maintain the main DC bus voltage within the targeted range.

## II. MODEL ANALYSIS

The MVDC power system on ships recommended by IEEE 1709 [7] was chosen to be the platform for testing the performance of the system and to assess the efficiency of the dynamic droop control. The simplified AES is shown in Fig. 1. The power on the ship is generated by two generators that meet the installed power demands. The two generators are connected to the main DC bus via AC/DC receivers. The two generators provide the power to the load evenly. Different types of loads are installed in the AES, including the propulsion load, ship service loads and pulse loads. In this model, the pulse loads represent the electrical weaponry system. The HESS is added to the system to supply the pulse loads. A dynamic droop control is used to arrange the charge/discharge in different energy storage devices.

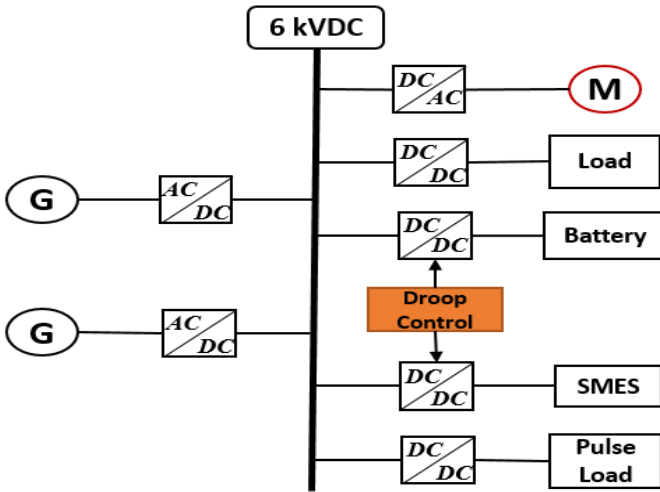


Fig. 1. Simplified AES including HESS.

### A. On-board Power Generation

There are several constraints on power generated by generators, including power equilibration limits, limits of the generator's active power, and the ramp-rate limits [17], [18]:

$$\sum_{j=1}^G P_{ij} = P_{Di} + P_{Li} \quad i = 1, 2, \dots, N \quad (1)$$

$$P_j^{min} \leq P_{ij} \leq P_j^{max} \quad i = 1, 2, \dots, N, j = 1, 2, \dots, G \quad (2)$$

$$\frac{P_i(n) - P_i(n-1)}{\Delta t} \leq k \quad (3)$$

where  $P_j^{min}$  and  $P_j^{max}$  are the upper and lower allowable active power outputs of generator  $j$ , respectively.  $P_i(n)$  and  $P_i(n-1)$  are the output power of the generator in two different moments  $\Delta t$ , and  $k$  is the allowable ramp-rate of the generator. Because the pulse load requires a high amount of power in a short period, and the ramp-rate of the generator cannot maintain it, the HESS is implemented in the system to supply this load. In our model, two diesel generators, 7 MW, 6.6 kV and 50 Hz, are modelled to generate power for the simplified AES.

### B. Electric Propulsion Motor

In this system, a synchronize motor is used as the electric propulsion motor. The propeller is connected directly to the synchronize motor. The mechanical load power of the motor is represented in (4):

$$P_{mec} = 2\pi nQ \quad (4)$$

where  $n$  represents the propeller rotational speed and  $Q$  is the torque of the propeller. The relationship between the supply frequency and the motor speed can be expressed as:

$$n = \frac{120f_r}{P} \quad (5)$$

where  $n$  represents the propeller rotational speed,  $f_r$  is the supply frequency and  $P$  is the number of motor poles. The power capacity of the propulsion motor is 2800 hp ( $\approx 2$  MW).

### C. Hybrid Energy Storage System

Because the ramp-rate of the generator is not high enough to supply and maintain the power demands of pulse loads, energy storage systems (ESS) have become essential to increase the amount of energy delivered within a short period. Two types of energy storage devices were chosen for this design: SMES and lithium-ion batteries. SMES is used as the high power density device to support the system during the transient periods. The SMES is controlled to deal with the short-term energy deficiency. The stored energy of SMES is calculated as follows:

$$E_{smes} = \frac{1}{2} LI^2 \quad (6)$$

Lithium-ion batteries are implemented in the AES to deal with long-term energy deficiency. Compared with other types of batteries, lithium-ion batteries have better energy density, low self-discharge and high efficiency [19], [20]. To protect the battery from overcharging and deep discharging, the state of charge (SOC) of the battery is regulated between 30% and 90% [21]. The design of the battery and SMES are based on the ship loads. There are three different types of load on the AES; 7 MW static load (ship service load), 2 MW motor load and 5 MW pulse loads. During the normal operation, the ship service load and the motor load are applied to the system with a total power demand of 9 MW. During the pulse load periods, the demand rises by 5 MW to a total of 14 MW. The battery capacity is

calculated by (7) at 13.88 kWh to cover the requirements of the pulse loads demand and to maintain the battery SOC constraints.

$$Battery_{cap} = \frac{Pulse\ loads * time\ (hour)}{SOC - (Upper\ Cont. + Lower\ Cont.)} \quad (7)$$

Because the SMES is more expensive than the Lithium-Ion battery in terms of energy density [19], the goal was to minimize the SMES size as much as possible whilst maintaining the voltage level at 6 kVDC. It was found that when the SMES size is reduced to < 500 kJ, a voltage drop occurred in the main DC bus before the battery began discharging. The design parameters of the AES are summarized in Table I.

TABLE I  
THE DESIGN PARAMETERS OF THE AES

Parameter	Quantity	Value
Generator	2	7 MW, 6.6 kV, 50 Hz
Motor	1	2800 hp ( $\approx$ 2 MW), 6.6 kV
Battery	Battery Bank	13.88 kWh, 92.53 kg, 0.0694 m <sup>3</sup> [22]
SMES	1	500 kJ ( $\approx$ 138.8 Wh), 17.35 kg, 0.69 m <sup>3</sup> [22]

### III. ENERGY STORAGE CONTROL METHOD

The main goal of this work is to design a dynamic droop control system to operate the HESS at better efficiency during pulse load periods. Previous studies demonstrated the droop control used to share different power sources [23], [24]. This paper proposes the use of HESS based on dynamic droop control to take advantage of the high power density of SMES and the high energy density of the battery in order to mitigate the effects of the pulse loads on the system's stability. The main principle of the control strategy is to generate different pulses in the SMES converter to control the charge and discharge of the SMES. The battery is controlled by a PI controller, which compares the main bus voltage and the voltage reference and considers the SOC of the battery. When the pulse load is added to the system, the SMES discharges immediately to feed the load and maintain the main bus voltage. Based on the dynamic droop control, the SMES discharge rate will decrease gradually to allow the battery to increase the discharge rate based on the pulses that are generated to the SMES and the battery. The main DC bus voltage is maintained within the required range ( $V_{ref(min)} < V_{bus} < V_{ref(max)}$ ). According to the IEEE standard [7], the DC voltage tolerance limits should be  $\pm 10\%$ . However, the tolerance limit was tightened to  $\pm 3\%$  in order to improve the system stability, as this was the main concern of this study.  $V_{ref(min)}$  is 0.97 pu of the nominal voltage, and  $V_{ref(max)}$  is 1.03 pu of the nominal voltage.

#### A. The SMES DC/DC Controller

The H-bridge DC/DC converter is used to control the charge and discharge of the SMES. It consists of two diodes (D1, D2), two MOSFETs (M1, M2) and an output capacitor, as shown in Fig. 2. There are three operation modes: the charge mode, the discharge mode and the standby mode. The charge/discharge

rate of the SMES is not only controlled by  $V_{ref}$ , but also controlled by the amount of the current stored in the SMES by (8) and (9). The goal of this control method is to change the charge and discharge rates of SMES based on the amount of the current stored in SMES to avoid the sharp charging and discharging. When SMES current decreases the discharge rate of the SMES decreases by (9), the voltage drop in the main DC bus slow down, thus the battery bank has more time to discharge to maintain the main DC bus at the required level. The three operation modes are shown in Fig.2.

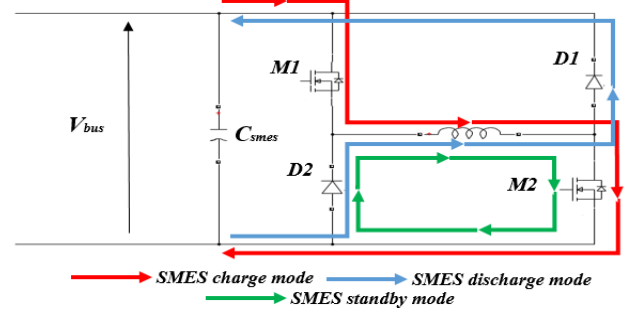


Fig. 2 The DC/DC H-bridge converter of SMES with three operation modes.

#### 1) ( $V_{bus} > V_{ref(max)}$ ) Charge mode

In charge mode, as shown in Fig. 2, the red directional arrows indicate that d1 (the duty ratio of M1) and d2 (the duty ratio of M2) are on, allowing the SMES to charge. At the same time, d1 receives another pulses according to (8) in order to decrease the charge rate of SMES gradually, allowing the battery to charge quickly. The two pulses are connected by the AND logical function, as shown in Fig. 3.

$$q = (k_a) \exp\left(\frac{I_{smes}}{k_{smes}}\right)^{k_b} \quad (8)$$

Where  $I_{smes}$  is the amount of the stored current in SMES,  $k_a$ ,  $k_b$  and  $k_{smes}$  are adjustable parameters that control the transition period between SMES and the battery based on  $I_{smes}$ .

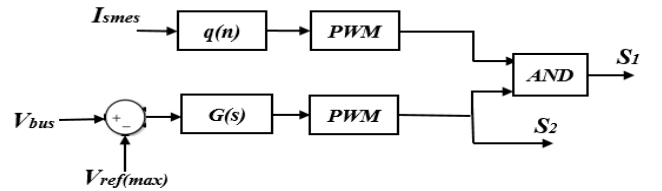


Fig. 3. Block diagram of the H-bridge DC-DC converter controller (charge mode)

#### 2) ( $V_{bus} < V_{ref(min)}$ ) Discharge mode

In discharge mode, d1 and d2 are off, allowing SMES to discharge through the two diodes as shown by the blue path in Fig. 2. At the same time, d2 receives another pulses, according to (9), to decrease the discharge rate of SMES gradually, allowing the battery to discharge quickly. The two pulses are connected by the OR logical function, as shown in Fig. 4.

$$q_2 = (k_a) \log_{10}\left(\frac{I_{smes}}{k_{smes}}\right)^{k_b} \quad (9)$$

Where  $I_{smes}$  is the amount of the stored current in SMES, and  $k_a$ ,  $k_b$  and  $k_{smes}$  are adjustable parameters that control the transition period between SMES and the battery based on  $I_{smes}$ .

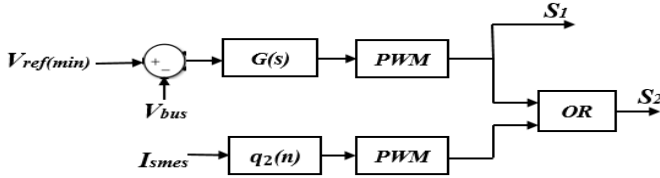


Fig. 4. Block diagram of the H-bridge DC-DC converter controller (discharge mode).

### 3) ( $V_{ref(max)} > V_{bus} > V_{ref(min)}$ ) Standby mode

In standby mode, the bus voltage is in the acceptable range between 0.97 and 1.03 pu of the nominal voltage. Hence, no output current from SMES is needed. To keep the current circulating between D2 and M2, d1 is off and d2 is on.

### B. The Battery DC/DC Controller

The half bridge DC/DC bidirectional converter based on the PI controller is used to control the battery charge and discharge. The converter consists of two IGBTs, Q1 and Q2, as shown in Fig. 5.

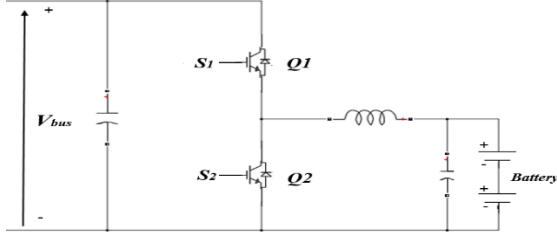


Fig. 5. DC/DC bidirectional converter based on PI controller.

In this control technique, the main DC bus voltage is compared with the reference voltage  $V_{ref}$  as shown in Fig. 6. The PI controller allows the battery to increase and decrease the charge and discharge rates based on the SMES current rate. When the SMES current starts to decrease by the dynamic droop control, the voltage starts to decrease slightly and the PI controller allows the battery to discharge and maintain the power demanded by the pulse load. The controller maintains the battery's SOC between 30% and 90%. More details pertaining to the battery DC/DC controller, the circuit and the control challenges can be found in [25], [26].

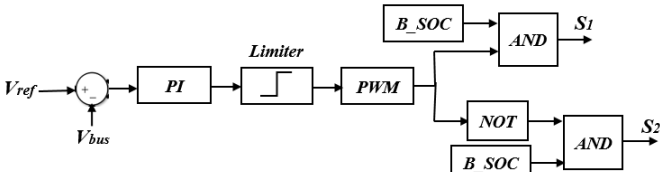


Fig. 6. Block diagram of the battery DC/DC converter controller.

## IV. SIMULATION RESULTS AND DISCUSSION

The simplified AES shown in Fig. 1 is modelled in the SimPowerSystems™ environment. The simulation results showed three different kinds of system behaviour: without ESS, with battery only and with HESS.

The simulation results demonstrated that the HESS based on the dynamic droop control showed good performance during

pulsed load periods, maintaining the main bus voltage at the required range and keeping the motor at the targeted speed. The system was subjected to pulse loads between  $t=4.0-7.0$  s and between  $t=10.0-13.0$  s. With the HESS, the minimum total generators capacity is 9 MW. However, without the HESS the minimum total generators capacity is 14 MW. The voltage of the main DC bus was 6 kVDC according to the IEEE standard [7].

In the conditions of without ESS and with battery only, when the pulse load was applied to the system at  $t=4.0$  s, the voltage dropped immediately to almost 3 kVDC. In the battery-only system, because the battery fed the pulse load, the voltage was regulated to the targeted level within a short period. However, in the HESS condition, the voltage remained stable at the targeted level throughout the test, both with and without pulse loads. In contrast, when the pulse load was removed at  $t=7.0$  s, the voltage increased rapidly because of the overcurrent. However, at the HESS, because the SMES absorbed the excessive current, the voltage stayed at the targeted level. Fig. 7 shows the comparison of the main DC bus voltage without ESS, with battery-only and with HESS.

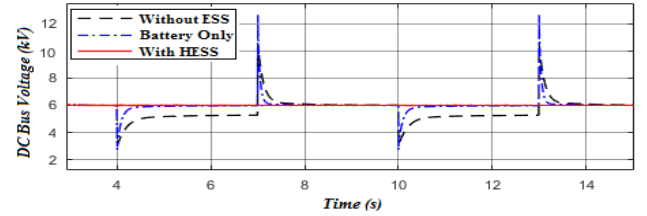


Fig. 7. The DC bus voltage without ESS, battery only system and with HESS.

Because the HESS was controlled to supply the pulse loads, the output power of the generators stayed constant at 9 MW with and without the pulse loads, as shown by the red line in Fig. 8.

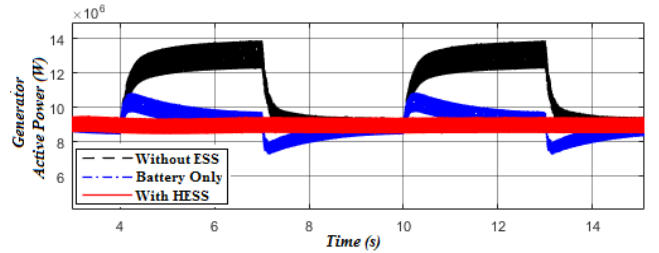


Fig. 8. The total power generation without ESS, with battery only and with HESS.

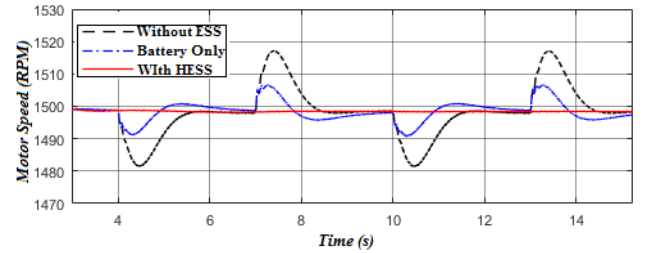


Fig. 9. The propulsion motor speed without ESS, with battery-only and with HESS.



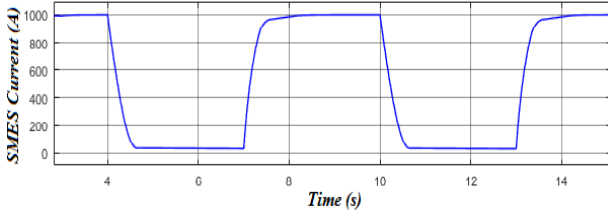


Fig. 10. SMES current.

In Fig.10, the maximum stored current in SMES is 1000 A. When the pulse load is applied to the system, SMES discharges immediately. It discharges 1000 A in 300 millisecond with a ramp-rate current of 3.3 kA/s. Because the discharge rate is controlled by both  $V_{ref}$  and  $I_{smes}$ , the discharge rate is decreased when SMES current decreased by (9). The goal of decreasing the discharge rate of SMES is to slow down the voltage drop in the main DC bus, thus giving more time for the battery to responds. Fig.11 shows the battery current. When the pulse loads are applied to the system, the SMES and the battery discharge to meet the sudden change loads demand at the beginning, then the battery becomes the main source of the power after SMES completely discharged. The current ramp-rate of the battery is 2.6 kA/s and the constant discharge current is 800 A. In special electrical applications, such as pulse load applications there are a few electrical devices that can supply high power in a short period, such as SMES and batteries. The Lithium-Ion batteries current ramp-rate can be reduced by increasing the size of SMES. However, a trade-off between the cost of the SMES and the battery life must be made. In future work, an optimization study will be done to find the optimum battery vs SMES size to have the best price for the ESS and battery life. In this work the main goal is to study the performance of the HESS and the energy storage control method under the sudden load changes.

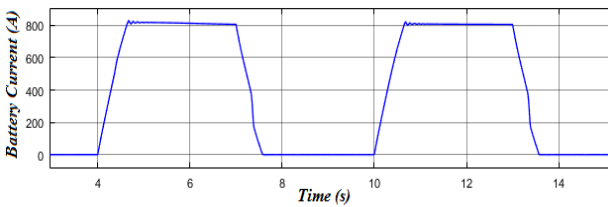


Fig. 11. Battery output current.

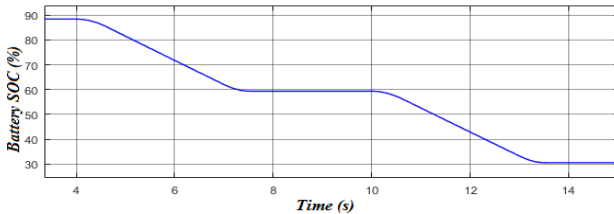


Fig. 12. Battery state of charge.

## V. CONCLUSION

This paper proposes the use of the SMES/battery HESS based on the dynamic droop control in the AES to mitigate the effects of the sudden load changes on the system's stability. The AES including SMES/battery was built in the SimPowerSystems™ environment to test the system's behaviour with and without HESS. The HESS based on dynamic droop control

showed good performance during the pulse load periods. By supplying the pulse loads from the HESS, the system maintained the voltage at the targeted level, keeping the motor at the required speed and maintaining constant generation output power both with and without pulse loads. To further investigate this approach, an experimental system containing a SMES and battery HESS will be constructed and tested in our laboratory. An optimization study for the SMES size and the battery life will also be performed.

## REFERENCES

- [1] M. Cupelli, *et al.*, "Power Flow Control and Network Stability in an All-Electric Ship," in *Proceedings of the IEEE*, vol. 103, no. 12, pp. 2355-2380, Dec. 2015.
- [2] Monti, A., *et al.*, "Energy storage management as key issue in control of power systems in future all electric ships." *Power Electronics, Electrical Drives, Automation and Motion, 2008. SPEEDAM 2008. International Symposium on.* IEEE, 2008..
- [3] Vu, Tuyen V., *et al.*, "Predictive control for energy management in ship power systems ..," *IEEE Transactions on Energy Conversion* (2017).
- [4] J. Lopez, "Combustion engine vs gas turbine—Ramp rate," Nov. 2016. [Online]. Available: Wartsila.com
- [5] N. H. Doerry and J. V. Amy, "The Road to MVDC," in *Proc. Intelligent Ships Symposium*, 2015.
- [6] J. F. Hansen and F. Wendt, "History and State of the Art in Commercial Electric Ship Propulsion, Integrated Power Systems, and Future Trends," in *Proceedings of the IEEE*, vol. 103, no. 12, pp. 2229-2242, Dec. 2015.
- [7] IEEE Recommended Practice for 1 kV to 35 kV Medium-Voltage DC Power Systems on Ships," in *IEEE Std 1709-2010*, vol., no., pp.1-54, Nov. 2 2010
- [8] T. Ise, M. Kita, and A. Taguchi, "A hybrid energy storage with a SMES and secondary battery," *IEEE Trans. Appl. Supercond.*, vol. 15, no. 2, pp. 1915–1918, Jun. 2005.
- [9] L. Trevisani, *et al.*, "Cryogenic fuel-cooled SMES for hybrid vehicle application," *IEEE Transactions on Applied Superconductivity*, 19(3), 2008-2011.
- [10] Cansiz, Ahmet, *et al.*, "Integration of a SMES–Battery–Based Hybrid Energy Storage System into Microgrids." *Journal of Superconductivity and Novel Magnetism* (2017): 1-9.
- [11] Lashway, Christopher R., Ahmed T. Elsayed, and Osama A. Mohammed. "Hybrid energy storage management in ship power systems with multiple pulsed loads." *Electric Power Systems Research* 141 (2016): 50-62.
- [12] M. M. S. Khan, M. O. Faruque and A. Newaz, "Fuzzy Logic Based Energy Storage Management System for MVDC Power System of All Electric Ship," in *IEEE Transactions on Energy Conversion*, vol. 32, no. 2, pp. 798-809, June 2017.
- [13] S. Kulkarni and S. Santoso, "Impact of pulse loads on electric ship power system: With and without flywheel energy storage systems," *2009 IEEE Electric Ship Technologies Symposium*, Baltimore, MD, 2009, pp. 568-573.
- [14] Mahlia, T. M. L., *et al.*, "A review of available methods and development on energy storage; technology update." *Renewable and Sustainable Energy Reviews* 33 (2014): 532-545.
- [15] Li, Jianwei, *et al.*, "Design/test of a hybrid energy storage system for primary frequency control using a dynamic droop method in an isolated microgrid power system." *Applied Energy* 201 (2017): 257-269.
- [16] Ibrahim, Hussein, Adrian Ilinca, and Jean Perron. "Energy storage systems—characteristics and comparisons." *Renewable and sustainable energy reviews* 12.5 (2008): 1221-1250.
- [17] H. M. Chin, C. L. Su and C. H. Liao, "Estimating Power Pump Loads and Sizing Generators for Ship," in *IEEE Transactions on Industry Applications*, vol. 52, no. 6, pp. 4619-4627, Nov.-Dec. 2016.
- [18] J. Zhang, Q. Li, W. Cong and L. Zhang, "Restraining integrated electric propulsion system power fluctuation using hybrid energy storage

- system," *2015 IEEE International Conference on Mechatronics and Automation (ICMA)*, Beijing, 2015, pp. 336-340.
- [19] Hadjipaschalis, Ioannis, Andreas Poullikkas, and Venizelos Efthimiou. "Overview of current and future energy storage technologies." *Renewable and sustainable energy reviews* 13.6 (2009): 1513-1522.
  - [20] Pickard, William F., Amy Q. Shen, and Nicholas J. Hansing. "Parking the power: Strategies and physical limitations for bulk energy storage in supply-demand matching on a grid whose input power is provided .." *Renewable and Sustainable Energy Reviews* 13.8 (2009): 1934-1945.
  - [21] Li, Jianwei, *et al.* "Design and test of a new droop control algorithm for a SMES/battery hybrid energy storage system." *Energy* 118 (2017): 1110-1122.
  - [22] Farhadi, Mustafa, and Osama Mohammed. "Energy storage technologies for high-power applications." *IEEE Transactions on Industry Applications* 52.3 (2016): 1953-1961.
  - [23] Shim, Jae Woong, *et al.* "Synergistic control of SMES and battery energy storage for enabling dispatchability of renewable energy sources." *IEEE Transactions on applied superconductivity* 23.3 (2013): 5701205-5701205.
  - [24] Li, Jianwei, *et al.* "Analysis of a new design of the hybrid energy storage system used in the residential m-CHP systems." *Applied Energy* 187 (2017): 169-179.
  - [25] Nie, Z., Xiao, X., Hiralal, *et al.* "Designing and Testing Composite Energy Storage Systems for Regulating the Outputs of Linear Wave Energy Converters." *Energies*, 10(1) (2017), p.114.
  - [26] Hussein, M., Senjyu, , *et al.* "Control of a Stand-Alone Variable Speed Wind Energy Supply System." †. *Applied Sciences*, 3(2) (2013), pp.437-456.